Multiferroicity in *B*-site ordered double perovskite Y_2MnCrO_6*

Fang Yong(房 勇), Yan Shi-Ming(颜士明), Qiao Wen(乔 文),
Wang Wei(王 伟), Wang Dun-Hui(王敦辉)†, and Du You-Wei(都有为)

National Laboratory of Solid State Microstructures and Key Laboratory of Nanomaterials of Jiangsu Province, Nanjing University, Nanjing 210093, *China*

(Received 18 May 2014; revised manuscript received 2 July 2014; published online 17 September 2014)

Double perovskite manganite Y_2MnCrO_6 ceramic is synthesized and its multiferroic properties are investigated. Novel multiferroic properties are displayed with respect to other multiferroics, such as high ferroelectric phase transition temperature, and the coexistence of ferrimagnetism and ferroelectricity. Moreover, the ferroelectric polarization of Y_2MnCrO_6 below the magnetic phase temperature can be effectively tuned by an external magnetic field, showing a remarkable magnetoelectric effect. These results open an effective avenue to explore magnetic multiferroics with spontaneous magnetization and ferroelectricity, as well as a high ferroelectric transition temperature.

Keywords: magnetism, ferroelectricity, magnetoelectric effect, multiferroics

PACS: 75.47.Lx, 77.80.–e, 75.85.+t **DOI:** 10.1088/1674-1056/23/11/117501

1. Introduction

In recent decades, there has been a great deal of interest in researching the magnetoelectric (ME) effect, which is led by the microscopic coupling of charge, lattice, and spin order, because of the fundamental curiosity of underlying physics as well as potential applications in multi-state memories, new functional sensors, and so on.[1–4] Due to such technological and fundamental aspects, knowledge of type-II multiferroics, in which ferroelectricity arises from spin, is highly desired, because type-II multiferroics show a large ME coupling effect.[1–4] Since the discovery of large ME coupling in $TbMnO_3$, a variety of materials with magnetic-induced ferroelectric polarization have been synthesized and extensively studied.[5–12] Two main microscopic theories have been reported that can account for the magnetically induced ferroelectricity, namely: the exchange striction and the spin current (inverse Dzyaloshinskii–Moriya) mechanism.[13–16] According to the former, ferroelectricity can arise via a symmetric exchange striction, which originates from the Heisenberg exchange interaction and induces local polarization P between two magnetic sites S_i and S_j in the form of $P \propto S_i \cdot S_j$, in collinear spin systems, such as $DyFeO_3$, Ca_3CoMnO_6, $GdFeO_3$, and $TbFeO_3$.[17–20] In the latter, the spin systems with cycloidal spiral magnetic structures can also develop finite polarization if the spin rotation axis $\hat{e}$ does not coincide with the propagation vector $\boldsymbol{Q}$, with $P \propto \hat{e} \times \boldsymbol{Q}$. This model illuminates the features of some noncollinear spin-induced ferroelectrics, such as $TbMnO_3$, $Ni_3V_2O_8$, $CoCr_2O_4$, and $MnWO_4$.[5,21–24] So far, magnetically-induced ferroelectric materials have been revealed in many systems. However, most of the discovered materials are antiferromagnets, which might limit potential applications due to the weak magnetism. Therefore, exploration of materials with ferroelectricity induced by a special spin structure with spontaneous magnetization is extremely crucial. Recently, theoretical and experimental results have demonstrated that spontaneous magnetism and considerable ferroelectric polarization can coexist in some double perovskite manganite materials, such as Y_2NiMnO_6, Lu_2CoMnO_6, and Y_2CoMnO_6.[25–27] Take Y_2CoMnO_6 for example. It is a Co–Mn ordered double perovskite with a ↑↑↓↓ spin structure, which is the precondition to develop ferroelectricity in this compound.[27] In this paper, we report our synthesis of the *B*-site ordered double perovskite manganite material Y_2MnCrO_6 and investigate its magnetic, ferroelectric, and ME behaviors in detail.

2. Experiments

Polycrystalline Y_2MnCrO_6 samples were synthesized via the standard solid-state reaction method.[28] The solid solution was prepared with a stoichiometric mixture of Y_2O_3 (dried at 1073 K for 12 h before use), Cr_2O_3, and MnO_2 powders as the precursor. The powders were carefully weighed and ground. The products were then pressed into pellets and sintered in air at 1173 K for 12 h. The pellets were then ground, re-pelleted, and sintered at 1473 K for another 12 h in air. After grinding again, the resulting powders were repressed into pellets and finally sintered at 1673 K for 30 h. The phase purity and crystallinity were characterized by X-ray diffraction (XRD) with Cu $K\alpha$ radiation at room temperature, using a Bruker XRD system (D8 Advance Davinci Bruker, Germany)

*Project supported by the National Basic Research Program of China (Grant No. 2009CB929501), the National High Technology Research and Development Program of China (Grant No. 2014AA032904), and the National Natural Science Foundation of China (Grant Nos. 11174130 and U1232210).

†Corresponding author. E-mail: wangdh@nju.edu.cn

© 2014 Chinese Physical Society and IOP Publishing Ltd

over a scanning range of Bragg angles $20^\circ \leq 2\theta \leq 80^\circ$ at the rate of 0.02° per step. The Rietveld refinement of the XRD profile was performed using the GSAS program. Magnetic properties were measured by a superconducting quantum interference device magnetometer (MPMS, Quantum Design). The pyroelectric current was collected with an electrometer (Keithley 6514) and a physical property measurement system (PPMS, Quantum Design). Before the measurements of the pyroelectric current, golden electrodes were sputtered onto the widest faces of the samples. Then, the samples were poled in an electric field $E = 667$ kV/m from 120 K to 2 K, after which the samples were short-circuited for a long-enough time to release any charge accumulated on the sample surfaces or inside the samples. The temperature dependences of the electric polarization were obtained by integrating the pyroelectric current upon warming.

3. Results and discussion

Figure 1 shows the XRD data and the Rietveld refinement of Y_2MnCrO_6, which suggests that the synthesized sample is a single phase with monoclinic space group $P2_1/n$. The room-temperature cell parameters of this compound, as obtained from the GSAS software, are as follows: $a = 5.260760$ Å, $b = 5.646837$ Å, $c = 7.485604$ Å, $\alpha = 90^\circ$, $\beta = 90.0262^\circ$, $\gamma = 90^\circ$. Table 1 presents the atomic coordinates, bond lengths, and bond angles of Y_2MnCrO_6 estimated from the room-temperature XRD. As evidenced, there are two distinct positions for Cr^{3+} and Mn^{3+}, and three inequivalent positions for the oxygen atoms (O_1, O_2, O_3) in the as-prepared polycrystalline Y_2MnCrO_6. The monoclinic crystal structure of Y_2MnCrO_6, which is similar to the double perovskite multiferroic material Y_2CoMnO_6, indicates that the Cr^{3+} and Mn^{3+} ions in the B sites are ordered.[27] As intuitively described in the inset of Fig. 1, the transition metal cations (Cr^{3+} and Mn^{3+}) occupy the center of the BO_6 octahedron and the Y cations are located between two consecutive layers, each of which is made up of a $GdFeO_3$-type distorted octahedron. Therefore, a B-site ordered crystal structure is obtained in Y_2MnCrO_6, which is important for producing ferroelectricity in this compound.[26,27]

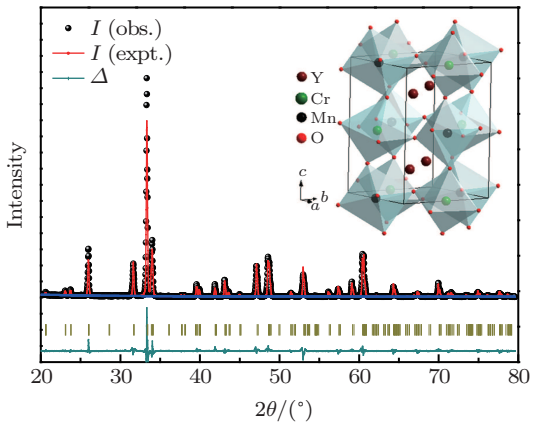


Fig. 1. (color online) XRD pattern and Rietveld refinement for Y_2MnCrO_6 at room temperature; the inset shows the crystalline structure of Y_2MnCrO_6, in which Cr^{3+} (green) and Mn^{3+} (black) ions reside at the oxygen polyhedron, Y^{3+} (brown) ions are situated between two $GdFeO_3$-type distorted oxygen polyhedral layers.

Table 1. Structural parameters of Y_2MnCrO_6.

Atom	X	Y	Z
Y	0.518019	0.573655	0.252743
Cr	0.000000	0.500000	0.000000
Mn	0.500000	0.000000	0.000000
O1	0.384000	0.958000	0.241100
O2	0.197000	0.195700	–0.057500
O3	0.322800	0.695300	–0.059300
Bond			Length/Å
Cr–O1			2.0456
Cr–O2			2.0523
Cr–O3			2.0729
Mn–O1			1.9199
Mn–O2			1.9868
Mn–O3			2.0066
Bond			Angle/(°)
Cr–O1–Mn			141.395
Cr–O2–Mn			145.635
Cr–O3–Mn			142.122

Figure 2 shows the temperature dependence of magnetization (M–T) for this polycrystalline sample under 0.1 kOe in both zero-field-cooling (ZFC) and field-cooling (FC) modes. The irreversibility between the ZFC and the FC M–T curves can be clearly seen. In the ZFC process, with decreasing temperature, the magnetization increases from 75 K and reaches a maximum at about 36.8 K. Upon further reducing the temperature, the magnetization drops rapidly, almost to zero. Upon warming, the magnetization in the FC mode decreases gradually, showing a transition from ferromagnetism to paramagnetism. The inverse of magnetic susceptibility versus temperature ($\chi^{-1} = H/M - T$) of Y_2MnCrO_6 is plotted in the inset of Fig. 2. The extrapolation of the inverse susceptibility data in the high temperature region gives a negative paramagnetic Curie temperature of -26.2 K, indicating that this compound is antiferromagnetic at its ground state. Moreover, in the FC process, the ferromagnetic behavior observed in this compound can be ascribed to field-induced sliding of the domain walls due to the nearness of ferromagnetic instability, similar to the magnetic properties of Y_2CoMnO_6.[27] Since the crystalline structure and the magnetic behavior of Y_2MnCrO_6 are identical with those of Y_2CoMnO_6, it is reasonable to speculate that the two compounds have the same magnetic structure. It has been reported that the $\uparrow\uparrow\downarrow\downarrow$ spin configuration of Y_2CoMnO_6 can induce ferroelectric polarization at its magnetic transition temperature, involving magneto-striction between domain boundaries.[18,26,27] So it is necessary to inves-

tigate the ferroelectricity in Y_2MnCrO_6 below the magnetic ordering temperature.

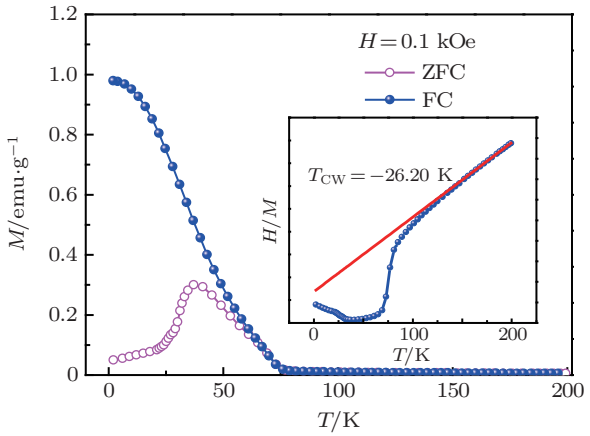


Fig. 2. (color online) Magnetization as a function of temperature measured under 0.1 kOe in ZFC and FC modes; the inset shows the temperature dependence of the inverse magnetic susceptibility.

Figure 3 shows the variation of the pyroelectric current as a function of temperature for Y_2MnCrO_6. A pronounced current peak is observed at 75 K, which is consistent with the magnetic transition temperature, indicating the close relationship between ferroelectric polarization and magnetism. In order to check the validity of ferroelectricity, we measured the temperature dependence of the pyroelectric current (I–T) with different warming rates: 2 K/min, 4 K/min, and 6 K/min, as indicated in Fig. 3. It is obvious that the peaks of the three I–T curves do not shift along the temperature axis and the integrals of the current for the three curves are almost identical (not shown), indicating that de-trapped charges, if any exist, do not contribute appreciably to the measured current and the intrinsic pyroelectric current is dominant. Moreover, we measured I–T under positive and negative poling electric fields ($E = \pm 667$ kV/m), respectively. The sign of the pyroelectric current can be determined by the external electric fields, as shown in the inset of Fig. 3, demonstrating the reliability of ferroelectricity in this compound.[29–31] As mentioned above, Y_2MnCrO_6 must have the same magnetic structure as Y_2CoMnO_6. In this spin configuration, the Cr^{3+} and Mn^{3+} ions form an Ising spin chain along the c axis and exhibit a staggered ↑↑↓↓ spin configuration. Between the regions with ↑ spins and those with ↓ spins, two kinds of domain walls develop in this compound: one locates at Cr^{3+}–Mn^{3+} and the other one locates at the Mn^{3+}–Cr^{3+} bond, as shown in the lower inset of Fig. 4. Through the magneto-striction induced by the domain walls, a slight structural distortion occurs and then induces ferroelectric polarization.[26,27] The two types of domain walls in this compound carry opposite polarizations and, due to the inequivalent cancellation, there must be a net polarization along the c direction. If the sample is cooled through its magnetic transition temperature under an electric field, it would store a net polarization by inducing more domain walls with one polarity than with the other.

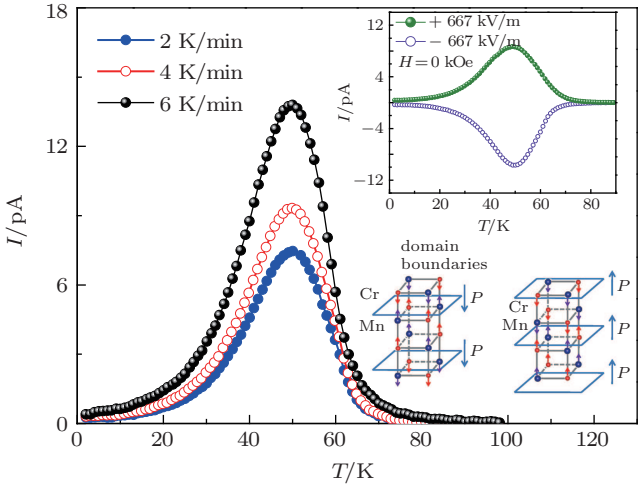


Fig. 3. (color online) Temperature dependence of the pyroelectric current under different warming rates: 2 K/min, 4 K/min, and 6 K/min. The upper inset plots the symmetric I–T curve under positive and negative poling electric fields. The lower inset schematically displays the ↑↑↓↓ spin structure along the c axis of Y_2MnCrO_6. Two scenarios (left and right) for the location of domain boundaries refer to regions sandwiched by ↑↑ and ↓↓ domains, along with two different directions of ferroelectric polarization.

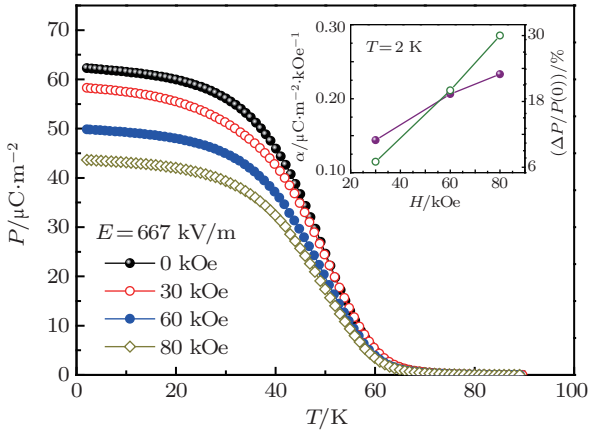


Fig. 4. (color online) Ferroelectric polarization as a function of temperature in the presence of various external magnetic fields; the inset shows ME coefficient α and change rate of polarization for Y_2MnCrO_6 at 2 K.

Both spontaneous magnetization and polarization can be observed at the same temperature, suggesting that an inherent coupling exists between them and the external magnetic field is likely to modify the ferroelectric polarization in Y_2MnCrO_6. In view of this, we measured the pyroelectric current of this sample under various magnetic fields (0 kOe, 30 kOe, 60 kOe, and 80 kOe) and obtained the polarization by integrating the current with time. A large spontaneous polarization of about 62.5 μC/m^2 is observed at 2 K, as is obvious in Fig. 4. With the application of the external magnetic field on the sample, the ferroelectric polarization is suppressed gradually, showing a remarkable ME effect. When the magnetic field is applied,

the regions with ↑ spins are larger than those with ↓ spins and the domain walls become less dense, suppressing the ferroelectric polarization.[27] In order to further evaluate the ME effect in multiferroic Y_2MnCrO_6, the magnetic field dependence of the ME coefficient $\alpha = \Delta P/\Delta H$ and the change rate of P ($\Delta P/P(0)$, $\Delta P = P(T) - P(0)$) at 2 K are plotted in the inset of Fig. 4. The two coefficients obviously increase in magnitude with increasing magnetic field, suggesting that the polarization responds strongly to the magnetic field. Comparing these two parameters of Y_2MnCrO_6 to those of Lu_2CoMnO_6 and Y_2CoMnO_6,[26,27] we find that the ME effect is enhanced in Y_2MnCrO_6.

4. Conclusion

In summary, we successfully synthesized the B-site (Cr^{3+} and Mn^{3+}) cation-ordered double perovskite Y_2MnCrO_6 by solid-state reaction. In this compound, ferrimagnetism and ferroelectric polarizations coexist and the ferroelectric polarization develops below its magnetic transition temperature, which suggests an intimate coupling between magnetic and ferroelectric orders. In addition, the ferroelectric polarization responds strongly to applied magnetic fields, showing a remarkable ME effect. It is argued that the polarization observed in Y_2MnCrO_6 can be ascribed to the breaking of the magnetic symmetry induced by the ↑↑↓↓ spin arrangement and the suppression of polarization by a magnetic field can be attributed to domain wall sliding under the external field. These observed ME effects in Y_2MnCrO_6 imply much underlying physics and have potential applications in the next generation of electronic devices with spontaneous magnetization and ferroelectric polarizations.

References

[1] Scott J F 2007 *Science* **315** 954
[2] Spaldin N A and Fiebig M 2005 *Science* **309** 391
[3] Eerenstein W, Mathur N D and Scott J F 2006 *Nature* **442** 759
[4] Béa H, Gajek M, Bibes M and Barthélémy A 2008 *J. Phys.: Condens. Matter* **20** 434221
[5] Kimura T, Goto T, Shintani H, Ishizaka K, Arima T and Tokura Y 2003 *Nature* **426** 55
[6] Prokhnenko O, Feyerherm R, Dudzik E, Landsgesell S, Aliouane N, Chapon L C and Argyriou D N 2007 *Phys. Rev. Lett.* **98** 057206
[7] Kimura K, Nakamura H, Kimura S, Hagiwara M and Kimura T 2009 *Phys. Rev. Lett.* **103** 107201
[8] Lee J H, Jeong Y K, Park J H, Oak M A, Jang H M, Son J Y and Scott J F 2011 *Phys. Rev. Lett.* **107** 117201
[9] White J S, Honda T, Kimura K, Kimura T, Niedermayer C, Zaharko O, Poole B, Roessli A and Kenzelmann M 2012 *Phys. Rev. Lett.* **108** 077204
[10] Murakawa H, Onose Y, Miyahara S, Furukawa N and Tokura Y 2010 *Phys. Rev. Lett.* **105** 137202
[11] Hwang J, Choi E S, Ye F, Dela Cruz C R, Xin Y, Zhou H D and Schlottmann P 2012 *Phys. Rev. Lett.* **109** 257205
[12] Tokunaga Y, Kaneko Y, Okuyama D, Ishiwata S, Arima T, Wakimoto S, Kakurai K, Taguchi Y and Tokura Y 2010 *Phys. Rev. Lett.* **105** 257201
[13] Katsura H, Nagaosa N and Balatsky A V 2005 *Phys. Rev. Lett.* **95** 057205
[14] Mostovoy M 2006 *Phys. Rev. Lett.* **96** 067601
[15] Sergienko I A and Dagotto E 2006 *Phys. Rev. B* **73** 094434
[16] Ishiwata S, Kaneko Y, Tokunaga Y, Taguchi Y, Arima T H and TokuraY 2010 *Phys. Rev. B* **81** 100411
[17] Tokunaga Y, Iguchi S, Arima T and Tokura Y 2008 *Phys. Rev. Lett.* **101** 097205
[18] Choi Y J, Yi H T, Lee S, Huang Q, Kiryukhin V and Cheong S W 2008 *Phys. Rev. Lett.* **100** 047601
[19] Tokunaga Y, Furukawa N, Sakai H, Taguchi Y, Arima T H and Tokura Y 2009 *Nat. Mater.* **8** 558
[20] Song Y Q, Zhou W P, Fang Y, Yang Y T, Wang L Y, Wang D H and Du Y W 2014 *Chin. Phys. B* **23** 077505
[21] Lawes G, Harris A B, Kimura T, Rogado N, Cava R J, Aharony A, Entin-Wohlman O, Yildirim T, Kenzelmann M, Broholm C and Ramirez A P 2005 *Phys. Rev. Lett.* **95** 087205
[22] Yamasaki Y, Miyasaka S, Kaneko Y, He J P, Arima T and Tokura Y 2006 *Phys. Rev. Lett.* **96** 207204
[23] Arkenbout A H, Palstra T T M, Siegrist T and Kimura T 2006 *Phys. Rev. B* **74** 184431
[24] Terada N, Khalyavin D D, Manuel P, Tsujimoto Y, Knight K, Radaelli P G, Suzuki H S and Kitazawa H 2012 *Phys. Rev. Lett.* **109** 097203
[25] Kumar S, Giovannetti G, van den Brink J and Picozzi S 2010 *Phys. Rev. B* **82** 134429
[26] Yáñez-Vilar S, Mun E D, Zapf V S, Ueland B G, Gardner J S, Thompson J D, Singleton J, Sanchez-Andujar M, Mira J, Bishop N, Senaris-Rodriguez M A and Batista C D 2011 *Phys. Rev. B* **84** 134427
[27] Sharma G, Saha J, Kaushik S D, Siruguri V and Patnaik S 2013 *Appl. Phys. Lett.* **103** 012903
[28] Yang L, Duanmu Q Y, Hao L, Zhang Z F, Wang X P, Wei Y Y and Zhu H 2013 *J. Alloys Comp.* **570** 41
[29] Zhang G Q, Dong S, Yan Z B, Guo Y Y, Zhang Q F, Yunoki S, Dagotto E and Liu J M 2011 *Phys. Rev. B* **84** 174413
[30] Dong X W, Dong S, Wang K F, Wan J G and Liu J M 2010 *Appl. Phys. Lett.* **96** 242904
[31] Yu H W, Liu M F, Li X, Li L, Lin L, Yan Z B and Liu J M 2013 *Phys. Rev. B* **87** 104404